Atmos. Chem. Phys. Discuss., https://doi.org/10.5194/acp-2018-100
Manuscript under review for journal Atmos. Chem. Phys.
Discussion started: 2 February 2018

Atmospheric Chemistry and Physics Discussions

Seasonal and diurnal variability in air pollutants and short-lived climate forcers measured at the Rwanda Climate Observatory

H. Langley DeWitt[1], Jimmy Gasore[1,3,4], Maheswar Rupakheti[2], Katherine E. Potter[1], Ronald G. Prinn[1], Jean de Dieu Ndikubwimana[3], Julius Nkusi[3], and Bonfils Safari[4]

[1] Massachusetts Institute of Technology, Center for Global Change Science, Cambridge, MA, USA

[2]Institute for Advanced Sustainability Studies (IASS), Potsdam, Germany

[3]Ministry of Education, Climate Secretariat, Kigali, Rwanda

[4]Unviersity of Rwanda, Physics Department, Kigali, Rwanda

Atmos. Chem. Phys. Discuss., https://doi.org/10.5194/acp-2018-100
Manuscript under review for journal Atmos. Chem. Phys.
Discussion started: 2 February 2018

Atmospheric Chemistry and Physics Discussions

Abstract

Air pollution is still largely unstudied in sub-Saharan Africa, resulting in a gap in scientific understanding of emissions, atmospheric processes, and impacts of air pollutants in this region. The Rwanda Climate Observatory, a joint partnership between MIT and the government of Rwanda, has been measuring ambient concentrations of key long-lived greenhouse gases and short-lived climate-forcing pollutants (CO_2, CO, CH_4, BC, O_3) with state-of-the-art instruments on the summit of Mt. Mugogo (1.586° S, 29.566° E, 2590 m above sea level) since May 2015. Rwanda is a small, mountainous, and densely populated country in equatorial East Africa, currently undergoing rapid development but still at less than 20% urbanization. The position and meteorology of Rwanda is such that the emissions transported from both the northern and southern African biomass burning seasons affect BC, CO, and O_3 concentrations in Rwanda. Black carbon concentrations during Rwanda's two dry seasons, which coincide with the two biomass burning seasons, are higher at Mt. Mugogo than in major European cities. Higher BC baseline concentrations at Mugogo are loosely correlated with fire radiative power data for the region acquired with MODIS satellite instrument. Spectral aerosol absorption measured with a dual-spot Aethalometer also varies in different seasons, likely due to change in types of fuel burned and direction of pollution transport to the site. Ozone concentration was found to be higher in air masses from southern Africa than from northern Africa during their respective biomass burning seasons. These higher ozone concentration in air masses from the south could be indicative of more anthropogenic emissions mixed with the biomass burning emissions from southern Africa as Rwanda is

downwind of major East African capital cities in this season. During the rainy season, local emitting activities (e.g., cooking, transportation, trash burning) remain steady, regional biomass burning is low, and transport distances are shorter as rainout of pollution occurs regularly. Thus local pollution at Mugogo can be estimated during this time period. Understanding and quantification of the percent contributions of regional and local emissions is essential to guide policy in the region. Our measurements indicate that air pollution is a current and growing problem in equatorial East Africa that deserves immediate attention.

1. Introduction

According to recent data collected and published by the World Bank, particulate air pollution in most African countries is above the annual average guideline values recommended by the World Health Organization (WHO). Despite this, little scientific research has been performed on air quality in Africa. The WHO reports that one in eight premature deaths globally can be linked currently to poor air quality, and these deaths are concentrated in developing countries (WHO, 2013). Black carbon (BC) is one of the major air pollutants emitted from Africa, mainly from biomass burning as it is widespread on the continent during certain seasons. In addition to affecting health, BC contributes to atmospheric heating and thus to climate change(Ramanathan and Carmichael, 2008). Widespread crop fires in northern and southern Africa, prevalent in boreal winter (December-January-February, DJF) and astral winter (June-July-August, JJA), respectively, are known to increase aerosol and ozone concentrations in this region and transported molecular and aerosol fire

tracers associated with elevated ozone have been measured as far as the Pacific and Indian Oceans (Field et al., 2016; Real et al., 2010).

In addition to biomass burning, recent work has pointed to diffuse and inefficient combustion emissions (DICE) from anthropogenic sources as having a significant effect on air quality in sub-Saharan Africa, and densely populated areas have higher DICE concentrations(Marais and Wiedinmyer, 2016). Examples of DICE include agricultural burning, trash burning, cook stoves, kerosene lanterns, brick kilns, charcoal making, vehicles, and diesel generators (Marais and Wiedinmyer, 2016). The rapid development of Africa, if not combined with development and enforcement of emission regulations and concurrent air quality monitoring, could lead to increased emissions of air pollutants and greenhouse gases from Africa to the global atmosphere in the near future as vehicle use, industry, generator use, and fossil-fuel power plants increase (Liousse et al., 2014). Past studies have suggested that pollution emitted near the equator has a larger impact on tropospheric ozone than pollution emitted in other regions due to consistent sunlight and heat available in the region to produce ozone (Zhang et al., 2016). Much of Africa's population is near the equator, and population density is one driver of DICE emissions. Collecting data on these diffuse emission sources is difficult, and continuous and highly time-resolved (one hour or shorter time resolution) on-ground data is scarce in both major cities and rural areas in East and Central Africa. While satellite data is beginning to fill the gap of column-integrated air quality approximations, these approximations often don't provide ground-level information on concentrations of pollutants, and even they do, they are associated with later uncertainties. Currently, South Africa has

the most extensive network of air quality monitoring networks and highest number of completed field campaigns of the sub-Saharan African countries (Sauvage et al., 2005; Tiitta et al., 2014). The studies in South Africa have found that satellite data, as currently understood, is not an ideal proxy for on-ground measurements as there can be poor agreement between the two types of measurements (remote column versus in situ boundary layer) (Hersey et al., 2015).

Due to logistics of long-term measurement and lack of in-country scientific capacity, most studies completed in East and Central Africa have been short-term studies focused on either near-roadway air pollution or exposure to PM and CO emissions from cook stoves (Galbraith, 2014; Gatari and Boman, 2003; Kinney et al., 2011; Knippertz et al., 2015; Mkoma et al., 2009; Ngo et al., 2015) These studies find highly variable levels of air pollution, with BC comprising a significant percentage of aerosol particles (Gatari and Boman, 2003; Kinney et al., 2011; Mkoma et al., 2009; Ngo et al., 2015). The daily averaged ambient PM10 (particulate matter 10 micrometers or less in diameter) concentrations varied in these studies from 7 to over 80 $\mu g\ m^{-3}$. This huge spread in aerosol concentrations measured in East Africa, varying due to season and location, demonstrates the need for long-term high-frequency measurements to fully understand the complexity of air quality issues in this region. Short-term studies do not capture seasonal changes in emissions and transport, very likely significant as large-scale biomass burning emissions mix with increasing urban and industrial emissions. Emission sources and source characteristics are certain to be different than those in Europe or North America,

making in-situ data essential to increase our understanding of emissions from Africa and also improve the accuracy of atmospheric models for Africa.

Located in east-central Africa, Rwanda is the second most densely populated African country, following Mauritius. Approximately 11.6 million people lived within its 26,338 square kilometers as of 2016. Urbanization remains low at 18% (World Bank, 2011) and the majority of the population is involved in subsistence agriculture, but this is changing quickly. The country is undergoing rapid development, averaging an 8% per annum growth during 2001-2015. Rwanda's industrial sector still remains undeveloped at this time and a low urbanization rate and high vehicular cost means that large and continuous traffic jams are not yet an issue. However, combustion emissions from other small but numerous diffuse sources, including the use of biomass as the primary cooking fuel by the majority of the population, are likely to be significant, particularly due to the high population density of Rwanda (Hersey et al., 2015; Marais and Wiedinmyer, 2016). These incomplete combustion emission sources, which emit CO and BC as well as other air pollutants, remain present and steady throughout the year (Bond et al., 2013). Many of these emissions lead to adverse health impacts. Lower respiratory infections are currently the largest single cause of death in Rwanda, leading to 11% of all deaths in 2015 and 17% of all deaths in children under five. Although these infections can't be directly traced to air quality, air quality is known to affect the respiratory health of children (IHME, 2016). This underscores air quality as a potential but unmeasured health risk in this region, as air quality is tied to lower respiratory disease, particularly in children (WHO, 2013).

To mitigate environmental problems often associated with rapid growth, the government of Rwanda has enacted a number of environmental regulations, including a ban on plastic bags, increased taxation on the importation of older vehicles, taxation of charcoal fuel within major cities, and age limits on motorcycles and buses brought in to the country for commercial use. Data on the effects of these current and future policies is needed for their justification and enforcement. The economic burden of regulation in this low-income country needs to be weighed against the lowering of health costs resulting from air quality improvement. Additionally, air quality issues in this region are not just restricted to individual countries, and overall increases in development and population density may be leading to a general increase in regional air pollution in east-central Africa.

Rwanda is located in the middle of the two major seasonal biomass burning regions of sub-Saharan Africa. Wide-scale biomass burning occurs to the north of Rwanda during December-January-February (DJF) and to the south during June-July-August (JJA). Rwanda's climate may exacerbate fire haze pollution effects, as Rwanda experiences two dry seasons that occur at the same time as these two continental burning seasons, making long range transport with low rainout efficiency likely. Rwanda's prevalent wind direction also changes from northerly (DJF) to southerly (JJA) at the same time as the large-scale biomass burning area shifts from north-central Africa to southern Africa. Increase in incidence and amount of biomass burning is thought to be one consequence of climate change in this region (Niang et al., 2014). Southern Africa's biomass burning is also influenced significantly by human activity, not just the climate (Archibald et al., 2010). Rwanda is positioned to

experience both large-scale (transported) haze due to fires and human activities and local, diffuse emissions.

In addition to air quality issues, climate change (related to air pollution) may also adversely affect Rwanda. The main products exported (coffee and tea), the livelihood of the majority of Rwandans (agriculture), and power (currently almost half of Rwanda's power is hydroelectric) are all potentially affected by climate change. These issues are similar across the region. Central Africa is expected to receive increased severe rainstorms, which may lead to erosion and an uptick in vector-borne diseases (Niang et al., 2014). However, there is limited on-ground data on air quality and climate change in Africa.

Therefore, in order to advance our scientific understanding of air pollution, climate change, and their impacts in Africa through generation of on-the-ground data, MIT and the government of Rwanda have established the Rwanda Climate Observatory (RCO) to measure long-lived greenhouse gases and short-lived climate forcers/pollutants in East Africa. Since May 2015, CH_4, CO, CO_2, O_3, and BC concentrations have been continuously measured, and N_2O measurements were added in February 2017.

The RCO is a part of the Advanced Global Atmospheric Gases Experiment (AGAGE) network, a global network of high-frequency trace greenhouse gas measurements (Prinn et al., 2000), and is the first station of its kind in Africa. Here we present first results on diurnal and seasonal variations in short-lived climate forcers/pollutants related to air quality, focusing on O_3, CO, and BC observed at the RCO. This dataset is unique and unprecedented to the region. We attempt to explain

seasonal differences in observed concentrations of these pollutants and their association with regional and local sources, meteorological conditions and repercussions for Rwanda. This information on overall concentrations, sources, and time-dependent concentration variations of these air pollutants is essential in this rapidly changing area of the world to not only advance our understanding of air pollution and climate change in the region but also inform future policies on air pollution with sound science.

2. Experimental Methods: Rwanda Climate Observatory

2.1 Rwanda Climate Observatory Environment

The RCO is located in the Northern Province of Rwanda, near Byangabo on the summit of Mt. Mugogo (1.586° S, 29.566° E, 2590 m above sea level). Mt. Mugogo is about 70 km (aerial distance) to the north-west from Kigali (population of approximately 1 million), 20 km (south-west) from the next major city, Musanze (population of around 100,000), and 60 km north-east from the Lake Kivu region (Gisenyi, Rwanda and Goma, DRC, combined population of approximately 1 million). A dirt road reaches the base of the mountain, about 500 m below the summit where the RCO is located, and a diesel generator is installed on the road at the base. Inlets were installed on both the roof of the Observatory (10 m above ground level) for O_3 and BC) and on a Rwanda Broadcasting Authority Tower (35 m above ground level) for CO, CO_2 and CH_4. There is a small Rwandan army camp adjacent to the measurement site and a eucalyptus forest and a mix of agricultural fields and scattered rural houses surround the immediate vicinity of the RCO (Figure 1). The high altitude and remote

positioning of Mt. Mugogo allows sampling of regional air masses from throughout East Africa depending on prevailing meteorological conditions, as well as local pollution (as the dense population but low urbanization of Rwanda means that direct human influence is everywhere except within the national parks).

2.2 Instrumentation

Details on the instruments sampling at the RCO are compiled in Table 1. PM2.5 BC (particulate matter 2.5 micrometers in diameter or less) was measured using a Magee Scientific 7-wavelength Aethalometer with dual-spot technology that is able to correct for filter loading artifacts (Drinovec et al., 2015). A cyclone PM2.5 impactor was installed on the inlet to remove larger particles. Air was passed through a filter once per day to collect blank data. Flow was calibrated once per year and after major instrument movement and changes, while the optical performance was calibrated with a neutral density filter kit once per year. Data was recorded every minute at a 5 liter per minute (LPM) flow rate and particles were captured on a quartz fiber filter tape. The air stream was not dried and the relatively humidity (RH) was not controlled, which could lead to increased uncertainty during periods of high relative humidity. RH recorded at the station varied by approximately 5% over the day and from 60-85% monthly, depending on the season. The 880 nm channel was used to calculate the concentration of BC.

CO mixing ratios were measured in real-time using a cavity ring-down spectrometer (G2401, Picarro, USA). Sampled, laboratory, and calibration air were dried with a Nafion drier inside an Earth Networks calibration box to increase the

accuracy of the Picarro water vapor correction (Welp et al., 2013). Three NOAA-standard calibration tanks were used for calibration spanning normal ambient concentrations and calibrations were performed once per day initially to check for linearity of instrument's response (Gasore, 2018). An O_3 monitor (T400, Teledyne Advanced Pollution Instrument, USA) was used to measure O_3. Regular checks were performed using internal span and zero O_3 calibrations. Flow was calibrated two to three times per year.

Meteorological data (ambient temperature, relative humidity, pressure, wind speed, wind direction and rainfall) were collected with an automatic weather station (WXT520, Vaisala, Finland). The weather station was attached to a fixed, hinged arm 35 m above ground level and connected to the communications tower, level with the $CO/CO_2/CH_4$ inlet, with a 2 m clearance from the tower.

3. Results and Discussion

Figure 2 shows the time series of 15 minute and daily averaged BC, O_3 and CO concentrations monitored at the RCO from May 2015 through January 2017. The 15 minute averaged data were used to further investigate daily, diurnal, weekly, monthly and season variations. The diurnal, weekly, and monthly variations in concentrations of each species, normalized to their average, are shown in Figure 3.

3.1 Seasonal Variation in BC, CO, and O_3

It has been known for some time that wide-scale biomass burning in sub-Saharan Africa has a large seasonal effect on the atmosphere (Archibald et al., 2010; Crutzen and Andreae, 1990). Understanding and separating these seasonal effects from anthropogenic emissions can be difficult without continuous data sets both

during and outside of this period, especially as both biomass burning and anthropogenic emissions in this region of the world emit BC, CO, and PM, and anthropogenic emissions contain O_3 precursors that increase O_3 formation. Needed on-ground measurements of various aerosol and gas-phase species associated with fire and anthropogenic emissions in Africa are scarce, but recently the US Embassies in Addis Ababa, Ethiopia, and Kampala, Uganda have begun continuously measuring PM2.5 concentrations. The raw data is collected and reported online on the OpenAQ platform (OpenAQ.org). This dataset on PM2.5 concentrations in major cities over different seasons in this region has been valuable in gaining basic insights into the seasonal characteristics of PM2.5 concentrations in the region (Figure 4). The PM2.5 concentrations in both these cities showed clear seasonal patterns, though the seasonal patterns differed at the two sites. Addis Ababa (Ethiopia) is much further north than Rwanda and Ethiopia is in general higher in elevation than Rwanda (though at 2355 m, not higher than the RCO) and closer to the Indian Ocean. In Addis Ababa, the dry season is also in DJF, but measured PM2.5 concentrations were low during this season. HYSPLIT back trajectory calculations confirmed that air masses during this time of the year originated over the ocean, not from the continent. JJA is the rainy season in Ethiopia; however, back trajectories confirmed that air masses originating from fires over Madagascar and southern Africa were likely transported to Addis Ababa at times and an enhancement of almost 20 $\mu g\ m^{-3}$ for the JJA monthly averages of PM2.5 was observed. Kampala, Uganda is close to Rwanda, near the equator, and has a long dry season during JJA and a short dry season during DJF. Rainy and dry season extrema are shown in the available Kampala PM2.5 data, with

an enhancement during February and JJA of around 15 to 25-30 μg m^{-3}, respectively, above PM2.5 concentrations during other months. However, in Kampala during all months measured, including the rainy season where little regional biomass burning influence is likely, monthly averages remained above the WHO recommendations for air pollution levels at daily averages of 25 μg m^{-3} or less and, despite having a lower population than Addis, were consistently higher in PM2.5 concentrations. South Africa has the most air quality monitoring stations of any sub-Saharan African country and results from these stations show a PM2.5 peak only in the southern burning season (JJA), not surprisingly missing transported pollution from the northern (DJF) burning season (Hersey et al., 2015).

From these data, though there are only two data points, it appears that African countries near the equator may be positioned to experience six months per year of transported regional fire haze, from both the northern and southern biomass burning seasons. This is a concerning public health issue as equatorial Africa is densely populated, which means that many people will be affected by transported pollution, and the higher population density will increase the local diffuse pollution emissions (e.g., cooking fires, diesel engines), exacerbating the problem of transported fire haze pollution with additional locally emitted pollution.

BC and CO data from the RCO were examined to probe seasonal changes in air pollution in Rwanda. Like Uganda, Rwanda has two rainy seasons roughly occurring in March-April-May (MAM) and September-October-November (SON), and two dry seasons during December- January-February (DJF) and June-July-August (JJA). This generalized definition and durations of the seasons are used the purpose of

288 comparing data for multiple years. They therefore don't represent exact onset and
289 withdrawal dates of each rainy and dry season, as these dates are different each year.
290 High variations in BC concentrations can be seen in the BC time series (Figure 2 and
291 Figure 3), ranging from below 100 to above 20,000 ng m^{-3}, with an average value of
292 1,700 ng m^{-3} (standard deviation: 1,600 ng m^{-3}). Peak concentrations corresponded to
293 dry seasons. Spikes in BC concentrations that lasted for less than 15 minute with
294 values higher than 25,000 ng m^{-3} were removed before conducting any further
295 analysis to eliminate BC sources in the direct vicinity of the RCO. CO and O_3 mixing
296 ratios also increased during the dry seasons compared to the rainy seasons.
297 To explore the sources of BC, CO, and O_3 at the RCO, seven-day HYSPLIT back
298 trajectories were run every 6 hours using NCEP/NCAR reanalysis meteorological data
299 (Kalnay et al., 1996). This analysis provided insights on the approximate origin and
300 trajectories of air masses before arriving at RCO measured at the RCO. These
301 HYSPLIT back trajectories were separated into DJF, MAM, JJA, and SON and are shown
302 with MODIS satellite fire count data colored by fire radiative power (FRP, W m^{-2})
303 (Figure 5). The MODIS fire count data and radiative power are used strictly for
304 qualitative, not quantitative, purposes in this work. Here we observe that, as major
305 biomass burning sites moved to the north and west in DJF, transport direction was
306 also primarily northerly, and as biomass burning move to Southern Africa in JJA, the
307 prevailing wind directions were also southerly. Although Rwanda itself had few large-
308 scale fires, its geographical position and meteorology meant that it experienced
309 transported fire haze from both major burn seasons. Black carbon measured at the
310 station tracked fairly well with summed daily FRP for sub Saharan Africa (Figure 5),

311 with R values varying from 0.75-0.10 depending on the month. Daily averages of BC
312 at the station often exceeded 5 μg m^{-3}, and the yearly average BC measured at the
313 station was greater than many rural measurement locations around the globe and on-
314 par with urban measurements in North America and Europe, though much lower than
315 measurements made in cities in China (Figure 6).

316 To further examine pollution transport to the RCO, the HYSPLIT back
317 trajectory geographical areas were gridded (using the R Openair package, (Carslaw
318 and Ropkins, 2012)) and merged, using date and time, with measured BC
319 concentrations and mixing ratios of O_3 and CO to generate concentration-weighted
320 back trajectories (cwt) for each season (more details on cwt available in (Hsu et al.,
321 2003; Seibert et al., 1994))(Figure 7). Trajectory time in each grid and arrival time of
322 each air mass were taken into account in this model to predict the likely source
323 regions and emission concentrations of pollutants measured at the RCO. This was
324 done to determine likely source regions of air pollution at the RCO by comparing
325 arrival times of air masses to the RCO and the time series of pollutants. This method
326 has proven fairly effective at identifying emission sources when comparing predicted
327 emission regions to emissions inventories (Lupu and Maenhaut, 2002) and is good as
328 a rough estimate of emission regions with no apriori information (Kabashnikov et al.,
329 2011). This method has low computational cost and is simple to set up, both of which
330 are important for areas with limited bandwidth or computational capacity and this
331 method can be repeated easily by in-country scientists.

332 BC and CO appeared to originate from similar areas, as expected due to their
333 overlapping sources of inefficient combustion and biomass burning. During JJA,

significant BC and CO appeared to originate from southern Africa and Madagascar, as well as from local sources near the RCO. During DJF, the source of these pollutants appeared to be much closer to the RCO, as major fires in the DRC and Uganda were also closer to the station. Throughout the measurement period, but particularly DJF, the Lake Kivu region also appeared to be a source of BC and CO. The Lake Kivu region is densely populated and use of both cook stoves and diesel generators is common.

In addition to direct emissions of BC and CO, other emissions such as volatile organic compounds and oxides of nitrogen from biomass burning are known to affect tropospheric O_3 concentrations, as they are precursors to O_3 formation (Jaffe and Wigder, 2012; Sauvage et al., 2005). It appears that such emissions likely played a role in the observed seasonal increase in O_3 mixing ratios of approximately 20 ppb in DJF and 25 ppb in JJA above rainy season levels at the RCO. The O_3 mixing ratio was highest during the JJA dry season, while BC had approximately the same monthly average concentrations in both dry seasons. This increase of about 5 ppb O_3 during JJA versus DJF was potentially due to the mixing of biomass burning emissions with anthropogenic emissions from east African cities such as Nairobi, Dar Es Salam, and Kampala during the JJA dry season. Direct source apportionment of O_3 is difficult as it formed downwind of emissions, but a mix of biomass burning and anthropogenic emissions from southern Africa could have been transported to Rwanda after photochemical aging and processing. During the DJF dry season, fires are closer to Rwanda and away from major urban areas. Fire haze air masses thus likely underwent less photochemical processing before arriving at the RCO and were exposed to less anthropogenic O_3 precursors. Increased stagnation or higher

temperature effects are unlikely to be driving this observation as wind speed is higher during JJA and temperature is similar or lower compared to DJF. During June and July, a loose correlation (R=0.47 and 0.45, respectively) between O_3 mixing ratios and BC concentrations was observed, while no correlations (R=-0.04, -0.15, and 0.07) were observed in December, January, and February.

The MOZAIC campaign in the late 1990s and early 2000s measured ambient O_3 mixing ratios at the Nairobi, Kampala, and Kigali airports and found Kigali, despite its smaller size and lower vehicle count, to have the highest O_3 mixing ratios among them (Sauvage et al., 2005). They measured a similar in magnitude increase in surface O_3 mixing ratios during the JJA season in Rwanda as our measurements at the RCO, although DJF was not measured in their work. Brazzaville, Republic of the Congo did report January and February O_3 measurements during the MOZAIC campaign. While much further west than Rwanda, in Brazzaville O_3 mixing ratios also increased during January and February, parallel to Rwanda, with monthly averages during January and February 25 ppb greater than the minimum of <30 ppb in April (Sauvage et al., 2005). This suggests influence from northern hemisphere biomass burning to O_3 mixing ratios at Brazzaville. Ozone in JJA at Brazzaville was almost 30 ppb higher than in January and February, however, so transport of air mass from the south and southern Africa biomass burning had a greater influence on O_3 in the region than transport from the north and biomass burning in central Africa. The 1992 SAFARI campaign also measured O_3 in sub-Saharan Africa throughout all seasons, and measured a seasonal ozone concentration peak during the JJA period for central and southern Africa (Thompson et al., 1996). A separate, large peak for DJF was not as observable

380 in the SAFARI data (Thompson et al., 1996). SAFARI measurements took place prior
381 to 1993, meaning that significant development in sub-Saharan Africa could have taken
382 place between the SAFARI campaign and the MOZAIC campaign (1997-2003) that
383 could drive the increasing O_3 in DJF as well as JJA over a period of almost a decade.
384 The SAFARI campaign measured the total column O_3, not the ground-level O_3 mixing
385 ratios, so data are not directly comparable.

386 The continuous collection of BC, CO and O_3 data during the dry and rainy
387 seasons allowed examination of both transported and local pollution in both seasons.
388 Here we define local pollution as pollution originating within twelve hours transport
389 time under typical wind speed conditions (<150 km, including both Rwanda and the
390 border areas with DRC and Uganda). During Rwanda's rainy seasons, the continental
391 fire count is also at a minimum, reducing large-scale biomass burning influence. The
392 region's emissions were from small-scale agricultural burning, charcoal making,
393 cooking fires, brick production (located in the valley below the station and throughout
394 the region), vehicles, diesel and heavy fuel-oil power plants, and diesel generators.
395 These activities continued throughout the rainy season and dry season at similar
396 rates.

397 The baseline daily average BC concentration in the rainy season remained at
398 0.5-1 μg m^{-3} after 12 hour periods without rain, which could be considered as
399 contributions of small but numerous diffuse emission sources to daily BC
400 concentration in this region. These values are not negligible, especially at a rural
401 location with little vehicular traffic or industries. If all BC during the rainy seasons is
402 assumed to be local in origin (within one day of transport, as typically rain occurs

each day during the rainy season), and this level remained the same throughout the year, yearly average contribution of local emissions to BC would vary between 18-100% of the total measured BC concentration at RCO-M. The shoulder months of September and February have been removed from this calculation as they have both rain and biomass burning influence, but on a yearly scale, around or greater than 35% of BC concentration measured at the station could originate from local (day transport) emissions, on par with previous estimates of the contribution of savanna and forest burning BC emissions versus other emission sources (Bond et al., 2013). While transported savanna, woodland, and forest fire emissions likely have a huge effect on Rwanda's air quality, targeting local emissions could bring a marked decrease in PM exposure of the population. More than 50% of BC measured in industrialized or densely populated areas of South Africa is modeled to be from anthropogenic emissions (Kuik et al., 2015). As Rwanda develops, its percentage contribution of anthropogenic BC could increase like South Africa's, if there is no regulation, on top of Rwanda experiencing 6 months a year of increased black carbon due to fire emissions (3 months more influence than South Africa experiences). In other words, it is necessary to reduce emissions from local sources within Rwanda to reduce exposure to air pollution but this will not be sufficient to reduce exposure to WHO recommended levels because Rwanda is significantly affected by large-scale regional biomass burning pollution as well, most occurring outside of the country.

3.2.1 Diurnal Variations in BC, CO and O_3

Diurnal variations in pollutant concentration of pollutants can provide important insights into information on local as well as regional pollution emission

426 sources. Diurnal variations in BC concentrations, CO mixing ratios and O_3 mixing
427 ratios observed at RCO in different by seasons are shown in Figure 8. At the RCO, the
428 O_3 mixing ratio exhibited a diurnal cycle with a peak in concentration in the evenings,
429 steady levels through the night and a minimum during mid-day. The increase of O_3 in
430 the evening is likely from regionally formed polluted air masses transported to the
431 station within the boundary layer and measured at the station during the collapsing
432 nocturnal boundary layer. Similar diurnal cycles were found at other mountain
433 locations remote from urban centers (Zhang et al., 2015). This diurnal pattern persists
434 in all seasons (Figure 8) and occurred on daily time scales, meaning that local urban
435 centers such as Kigali and Kampala were likely the source regions for this observed
436 daily increase in ozone. However, the differences in diurnal minima and maxima were
437 highest in the June-August period, and lowest in the December-February period. This
438 difference may be due to the differences in biomass burning proximity (far in JJA,
439 closer in DJF) and primary wind direction (southerly versus northerly). Flatter ozone
440 profiles generally indicate that ozone was neither produced locally nor heavily
441 influenced by daily variations in boundary layer height; as large-scale biomass
442 burning occurs closer to the RCO in DJF, O_3 may be more well-mixed within the
443 polluted mixed layer and have less time to be transported to higher altitudes in
444 troposphere as in JJA. Wind speed was similar during all months, and RH was similar
445 for DJF and JJA.

446 BC had mid-morning and early evening peaks that coincided with both cooking
447 times and kerosene/generator use times. The evening peak was higher, likely due to
448 more use of generator and kerosene lanterns for lighting in the evening (dark at 6

449 pm) than the morning (light at 6 am). These peaks persisted throughout the rainy and
450 dry seasons, indicating influence of local sources for these diurnal peaks. In the rainy
451 seasons, the average difference between minimum and maximum BC concentration
452 was around 0.5 μg m^{-3} and slightly higher (0.6 μg m^{-3}) in the dry season. During June-
453 August, we observed a general increase in BC concentrations in the morning hours,
454 while December-February, the morning had lower BC concentrations and the main
455 peak was observed in the evening with a small second peak in mid-afternoon. CO
456 mixing ratios had a similar but less pronounced diurnal variation. Like with O_3,
457 changing boundary layer conditions also likely played a role in variations in BC
458 concentrations over the day, as local boundary layer height increased during the day
459 and decreased during the evening and morning hours, and the RCO altitude was above
460 the boundary layer height often during the evening.

461 **3.3 BC source apportionment**

462 It is important to understand the pollution emission sources in East Africa,
463 beyond large-scale biomass burning, in order to enact policies and actions to reduce
464 these emissions. Past observational as well as atmospheric simulation studies show
465 that BC from biomass burning is the major source of pollution in this region(Andela
466 and van der Werf, 2014; Bond et al., 2013; Hersey et al., 2015; Marais and
467 Wiedinmyer, 2016; Sauvage et al., 2005), though fossil fuel BC emissions are
468 increasing with increasing socio-economic development activities (Knippertz et al.,
469 2015; Liousse et al., 2014). Regional emission models predict that only 10% of fuel
470 (by mass) burned in East Africa is fossil fuel (Marais and Wiedinmyer, 2016). Fuel
471 demand information from the Rwanda Bureau of Statistics and Ministry of

Infrastructure confirm <10% fossil fuel use is a reasonable amount for Rwanda, with demand of fuel wood for both charcoal making and direct burning is 4.2 billion kg and petroleum products is 287 million kg per year (wood use from 2016, fossil fuel use extrapolated from statistics in 2011/12 using a 10% per annum growth rate, fuel use summarized in Table 2)(Rwanda Ministry of Infrastructure, 2015). In regards to demand of petroleum products, diesel is the highest (46%) followed by petrol (31%), heavy fuel oil (12%), kerosene (6%), and jet-A fuel (5%). As of November 2016, approximately 27% of Rwanda's on-grid power generation (52 MW out of 190 MW) was either heavy fuel oil or diesel-derived (http://www.reg.rw/index.php/our-business/generation/624-power-generation-2), the rest is a mix of hydroelectric power (44%), methane gas (16%), solar, (5%) and imports from nearby countries.

While the majority of fuel use is wood, BC emission factors per kg fuel burned are different for open burning, three stone fires, and diesel generators and other engines using unregulated fuel in inefficient burning conditions (average approximations of EF is 0.75, 1, and 4 g kg^{-1}, respectively)(FAO, 2010). As there are less than 180,000 registered motor vehicles (including truck and motorcycles) in Rwanda, and less than a third of the power generated in-country is from fossil fuel, but over 2 million households use wood fuel for cooking, understanding the relative contribution of each emission source to black carbon particulates is essential to guide policy and development in the short-term. A four-times greater emission factor per unit of fuel burned, even for fuel that only comprises 10% of the total fuel use in-country, could make motor vehicle and diesel generator emissions a good first target. However, burning conditions, fuel conditions, and engine combustion conditions

(including presence or absence of a diesel particle filter, age of the engine) can greatly influence these emission factors. One way separation of fossil fuel combustion versus biomass burning BC particulate has been estimated in the past is by measuring the color of the particles (wood smoke particles have enhanced absorption in the UV, while fossil fuel combustion particles have flat absorption over all wavelengths)(Kirchstetter and Thatcher, 2012; Sandradewi et al., 2008).

The Aethalometer's seven wavelengths allow measurement of the wavelength-dependent aerosol absorption coefficients that can be used to infer the potential sources of BC aerosol (Drinovec et al., 2015; Sandradewi et al., 2008) measured. Theoretically, from the wavelength dependence of aerosol absorption, BC from fossil fuel and wood smoke can be differentiated(Sandradewi et al., 2008). Though this two-component model can provide a valuable knowledge on knowledge on source attribution of BC this model has some limitations. This model is more accurate if calibrated to local conditions(Dumka et al., 2013; Harrison et al., 2012), as different fuels and wood biomass burning creates aerosol with different radiative properties and the standard model, based on European studies, has been shown to be less applicable in developing countries (Garg et al., 2016).

From the Aethalometer data, wavelength dependence of absorption coefficients and the absorption Ångstrom exponent (AAE) were calculated and compared to literature values of different type of biomass burning and fossil fuel combustion. The AAE is a dimensionless property commonly used to characterize the wavelength-dependent absorption of BC and gives clues on the source and/or aging of BC when compared to laboratory and other ambient studies(Chung et al., 2012; Lack

and Langridge, 2013; Russell et al., 2010; Yuan et al., 2016). The AAE values assigned for the standard Aethalometer model separating the BC from biomass burning and fossil fuel combustion are two and one, respectively (Kirchstetter et al, 2004; Sandradewi et al, 2012; Drinovec et al. 2015). In this work, standard mass absorption cross-sections (MACs) for each wavelength provided by the manufacturer of the Aethalometer were used to calculate the absorption coefficient (b_{abs}) at each wavelength. For pure BC from fossil fuel, $b_{abs} \sim 1/\lambda$ and the AAE between two wavelengths (470 nm and 950 nm) is 1 using the equation $\ln(_{babs}\lambda_1/b_{abs}\lambda_2)/\ln(\lambda_2/\lambda_1)$. The average AAE (averaged for entire measurement period between July 2015 and January 2017) was calculated to be 1.65 (+/- 0.14) at the RCO using the 470 and 950 wavelength absorption and MACs (Figure 9)(Sandradewi et al., 2008; Drinovec et al. 2015). These wavelengths were chosen as the AAE calculated from 470 and 950 is generally comparable with other literature values(Saarikoski et al., 2012). The calculated AAE values were on par with AAE calculated from measurements taken in areas heavily influenced by biomass burning (Chung et al., 2012; Lack and Langridge, 2013; Russell et al., 2010; Saleh et al., 2013; Sandradewi et al., 2008; Yuan et al., 2016). Past studies have reported an AAE of 1.2-2.5 for biomass burning aerosol(Andreae and Gelencsér, 2006; Chung et al., 2012; Russell et al., 2010; Saleh et al., 2013, 2014). While daily only small variations (+/- 0.05) for AAE were observed, significant seasonal differences in this value were found, with monthly averaged values ranging from 1.5 (dry season) to 1.9 (at the end of the long rainy season). Studies in southern Africa measuring savanna and crop burning found an AAE of around 1.45 for ambient black carbon aerosol, and in the dry season savanna and crop

burning are the prevalent type of large-scale biomass burning in sub-Saharan Africa (Russell et al., 2010). The AAE calculated from the Aethalometer data at the RCO was higher during the rainy season when local emissions dominated our measurements. Eucalyptus burning, the most prevalent burning near the station (for charcoal making, cooking fires, brick kiln fuel) was measured in laboratory experiments to have a higher AAE than savanna burning (AAE of 1.71 +/- 0.50 calculated between 405 and 781 nm wavelengths)(Chung et al., 2012). Eucalyptus trees and savanna burning were certainly not the only two types of solid biofuel influencing measurements at the station, but the difference in AAE of aerosols produced from different fuels means that the AAE will have large variations based on fuel wood or other biomass used and this was reflected in our data.

Using the Aethalometer model with standard inputs not accounting for the different types of fuel used in East Africa versus Europe, a high influence of fossil fuel black carbon emissions was calculated: in the dry season, over 50% of black carbon was assigned to be fossil fuel in origin. Fossil fuel emissions certainly influenced the pollution at the RCO, as air masses from Kigali, Kampala, Nairobi, and Dar es Salaam were likely transported to the station and these cities likely have high black carbon emissions from generators, fossil fuel power stations, and older diesel vehicles but would also have significant biomass cook stove emissions (Gatari and Boman, 2003; Koch et al., 2009; Mkoma et al., 2009; van Vliet and Kinney, 2007). However, this number is likely falsely high: at <10% fuel demand of fossil fuel (all types) versus >90% wood and charcoal fuel demand, even if the g BC per kg fuel from diesel was 4x higher, and all fossil fuel use was unregulated diesel (unlikely), well under half of the

measured BC would be from fossil fuel combustion emissions. Additionally, the AAE calculated in all seasons had a flat diurnal profile, suggesting no daily change in aerosol source (e.g., rush hour traffic from Kigali) was measured at the RCO.

In order to gain more insights into the sources of BC we also examined the BC:CO over time. CO is also released by inefficient combustion and the ΔBC: ΔCO ratio can be different for different emission sources. In order to calculate this ratio we first converted the CO mixing ratios to concentrations (in $\mu g\ m^{-3}$), and then subtracted the 95^{th} percentile values for CO and BC from their respective concentrations. For the entire data set, the ΔBC: ΔCO (both in $\mu g\ m^{-3}$) ratio was 0.014 (R^2 0.79, n = 40523). The ΔBC: ΔCO ratio varied seasonally, with monthly average peaks reaching 0.016 in December, February, and July and lows below 0.01 in April. The average ratio of 0.014 for the measurement period was almost twice as high as in biomass burning plumes sampled over West Africa in an aircraft campaign (0.0072)(Moosmüller and Chakrabarty, 2011) but on par with or lower than measurements taken during the INDOEX campaign in the Indian Ocean (Dickerson et al., 2002). A study in Germany and Mexico found a correlation between diesel vehicle use and higher BC:CO (Baumgardner et al., 2002), while other studies have also found an increased ΔBC: ΔCO during periods more influenced by biomass burning (Pan et al., 2011). A study in India found no correlation in biomass-burning and fossil fuel-influenced ΔBC:ΔCO air masses (Sahu et al., 2012), as there are a wide range of ratios measured from the same source (Dickerson et al., 2002; Sahu et al., 2012). The high ΔBC:ΔCO ratio at the RCO could be due to the prevalence of older diesel engines in the country, which emit more BC to CO than newer engines (Cai et al., 2013), but, as the highest

587 value occurs during the Rwanda dry seasons and the continental biomass burning
588 seasons , likely the ratio is governed in part by rainout as BC is more easily removed
589 by wet deposition than CO. In this study, we were not able to use this ratio to further
590 separate biomass burning BC from fossil fuel combustion BC, likely due to differences
591 in emission profiles in developing versus developed countries. This underscores the
592 need for more measurements in East Africa to understand emission sources and
593 profiles and develop more-robust emission source profiles.

594 **4. Conclusions**

595 In this work, we present the first long-term and highly time-resolved
596 continuous measurements of short-lived climate forcers for a nearly two-year period
597 from July 2015 to January 2017 at the Rwanda Climate Observatory located at Mt.
598 Mugogo in Rwanda, in one of the data poor regions of the world. From these
599 observations, we find that:

600 1. During Rwanda's two dry seasons, the country experienced pollution
601 transported from both the northern (DJF) and southern (JJA) biomass
602 burning seasons in Africa. This transported pollution led to high black
603 carbon and carbon monoxide levels at the RCO, surpassing
604 concentrations measured in many major cities elsewhere. Emissions
605 from large-scale crop and savanna fires appeared to have a wide-
606 reaching effect on this region, reflected in increased PM2.5 in
607 Kampala, a major East African city, for both biomass burning seasons
608 and likely driving the increased O_3 measured during DJF and JJA by
609 our study and by past studies in equatorial Africa. The dense

610 population of equatorial East Africa and the double impact of the two
611 fires seasons could lead to significant public health problems for the
612 population in Rwanda and equatorial East Africa as exposure to
613 elevated levels of PM2.5 and BC concentrations occurs six months out
614 of the year.

615 2. Ground level O_3 was enhanced during both dry seasons, likely due to
616 the prevalent wide-scale biomass burning. Increased enhancement
617 was observed during the JJA dry season when the air masses
618 originated from the southeast and likely included a mix of biomass
619 burning and anthropogenic emissions (cooking fires, vehicles,
620 industries), leading to higher ozone concentrations at the RCO
621 downwind of these mixed pollution sources. As this area develops
622 and population grows, local as well as regional air pollution could
623 become a major environmental and societal issue that could be a
624 threat to national development goals.

625 3. Local emissions beyond large-scale biomass burning influence were
626 constant and estimated to contribute between 18-almost 100 % of
627 the measured black carbon concentrations depending on season, if
628 black carbon during the rainy season was assumed to be completely
629 local (Rwanda and neighboring countries) in origin (ranging from
630 0.5-1 μg m^{-3} daily average measured BC). These local emissions, from
631 different combustion sources (e.g., cooking fires, inefficient diesel
632 generators and engines with sub-standard fuel use, solid biomass fuel

633 burning, small agricultural fires), are likely concentrated in the
634 densely populated Rwanda and Lake Kivu economic area. Rwanda's
635 population is growing quickly and, as these local emissions are
636 related to population density, air pollution will likely increase unless
637 there is government intervention.
638 4. Different combustion fuel and burning practices in Europe and East
639 Africa calls into question the accuracy and applicability of a two-
640 component model for estimating BC from fossil fuel combustion and
641 biomass burning using AAE approximations for biomass burning and
642 fossil fuel combustion aerosol measured in Europe for use in East
643 Africa. There may also be different mass absorption cross-sections
644 for aerosols measured at the RCO than in Europe or North America.
645 This shows the need for multiple on-ground measurements to fully
646 understand pollution sources in different regions of the world,
647 notably in Africa. However, seasonal variations in the wavelength
648 dependence of ambient BC particles did point to different sources of
649 BC particles and this should be further explored in future studies.
650 5. The measurements we have provided in this study will be useful in
651 advancing atmospheric science in Africa, improve emission
652 inventories and air pollution/atmospheric models in the region, and
653 designing mitigation measures in the region, which has limited long-
654 term and in-situ atmospheric data.
655

These data and analyses, while acknowledging the high influence of regional biomass burning, also show that significant decreases in air pollution could be achieved within eastern and central Africa with targeted local policies, emphasizing cleaner diesel vehicles and generators, reduced wood-fuel reliance for cook stoves, and improved cook stoves to burn biomass fuel more efficiently. Currently, over 2 million households in Rwanda rely on wood burning (including charcoal) for cooking. While reducing this number will have significant economic costs, putting in place infrastructure for alternative cooking fuels (pellet stoves, LPG stoves, electrical stoves) could help the country avoid even higher local air pollution emissions and associated adverse impacts as the population grows. Diesel-fueled minibuses, common transport between towns in Rwanda and within Kigali, and older diesel vehicles are also high emitters of black carbon but newer vehicles with emissions control technology may be economically beyond the reach of local bus companies and citizens. Continuing to grow electrical capacity and connection will reduce the use of kerosene lanterns and diesel generators, and will reduce air pollution if additional energy capacity is achieved through renewable sources (solar, hydropower). The huge influence of regional biomass burning, exacerbated by equatorial East Africa's meteorology, and the potential influence of anthropogenic emissions from major cities on O_3 formation in this regions must also be examined as this area develops and this should be an important agenda for the regional discussions on environmental, public health, and other development issues.

6. Future Work

679 The government of Rwanda is working to establish an air quality and climate
680 change monitoring network throughout the country to measure ambient criteria air
681 pollutants and other key climate change related components of atmospheric pollution.
682 Building knowledge of air quality and climate change related emissions in this data-
683 poor area of the world is essential to fill the large data and knowledge gap in this
684 region. Adding ground-based measurements, comparing measurements to satellite
685 data, using data to evaluate and improve existing emission inventories, improving
686 accuracy of global/regional air quality and climate change models, and using data for
687 quantification of impacts of air pollution and climate change will help local
688 governments design appropriate mitigation strategies rooted in data and local
689 context.

690 **7. Data Availability**

691 This data will be made available at the AGAGE website,
692 https://agage.mit.edu/data/agage-data. All data used in this article will be made
693 available as of publication and data from this project on a rolling basis after quality
694 control.

695 **Acknowledgments:**

696 We thank the generous MIT alumni donors to the MIT-Rwanda Climate Observatory
697 Project that provided the funds to purchase, develop and install most of the
698 instruments at the Rwanda Climate Observatory. Additional funds for this purpose
699 were provided by the MIT Center for Global Change Science. COMESA provided the
700 funds to purchase and install the Aethalometer at the RCO. We also thank the
701 Government of Rwanda and the Rwanda Ministry of Education, specifically Mike

Hughes, Vianney Rugamba, and Dr. Marie Christine Gasingirwa, for supporting this project, including funding the staffing and infrastructure costs of the Rwanda Climate Observatory and the University of Rwanda for providing laboratory space and infrastructure for instrument testing. We thank Dr. Arnico Panday who provided guidance during the initial stages of this project. We also wish to acknowledge the essential contributions of the Mugogo station technical experts Theobard Habineza, Modeste Mugabo, Olivier Shyaka, and Gaston Munyampundu, and RBA technician Yves Fidele, without which running this station would be impossible.

Atmos. Chem. Phys. Discuss., https://doi.org/10.5194/acp-2018-100
Manuscript under review for journal Atmos. Chem. Phys.
Discussion started: 2 February 2018

712 Table 1: Instruments used in this study and measurement period used for analysis

INSTRUMENT	SPECIES MEASURED	MEASUREMENT PERIOD	TIME RESOLUTION
PICARRO G2401 CAVITY RING DOWN SPECTROMETER	CO_2, CO, CH_4, H_2O	MAY 2015-JANUARY 2017	1 MIN
MAGEE SCIENTIFIC AE33 7-WAVELENGTH AETHALOMETER	BLACK CARBON (PM2.5, CYCLONE IMPACTOR ON INLET)	MAY 2015-JANUARY 2017	1 MIN
TELEDYNE T400 API	O_3	MAY 2015-JANUARY 2017	1 MIN
VAISALA WXT	MET PARAMETERS (RH, WS, WD, T, P)	JULY 2015-JANUARY 2017	1S

Table 2:

Fuel Demand in Rwanda (2016, Rwanda Ministry of Infrastructure)

Fuel Type	Demand
Petrol	120442 kL
Diesel	178529 kL
Kerosene	22288 kL
Heavy Fuel Oils	59292 kL
Jet-A	18235 kL
Wood (charcoal + natural)	4,200,000 metric tons

719 References
720
721 Andela, N. and van der Werf, G. R.: Recent trends in African fires driven by cropland
722 expansion and El Niño to La Niña transition, Nat. Clim. Chang., 4(9), 791–795,
723 doi:10.1038/nclimate2313, 2014.
724 Andreae, M. O. and Gelencsér, A.: Black carbon or brown carbon? The nature of light-
725 absorbing carbonaceous aerosols, Atmos. Chem. Phys., 6(3), 3419–3463,
726 doi:10.5194/acpd-6-3419-2006, 2006.
727 Archibald, S., Nickless, A., Govender, N., RJ., S. and Lehsten, V.: Climate and the inter-
728 annual variability of fire in southern Africa: a meta-analysis using long-term field
729 data and satellite-derived burnt area data, Glob. Ecol. Biogeogr., 19(6), 794–809,
730 2010.
731 Baumgardner, D., Raga, G., Peralta, O., Rosas, I., Castro, T., Kuhlbusch, T., John, A. and
732 Petzold, A.: Diagnosing black carbon trends in large urban areas using carbon
733 monoxide measurements, J. Geophys. Res. Atmos., 107(21),
734 doi:10.1029/2001JD000626, 2002.
735 Bond, T. C., Doherty, S. J., Fahey, D. W., Forster, P. M., Berntsen, T., DeAngelo, B. J.,
736 Flanner, M. G., Ghan, S., Kärcher, B., Koch, D., Kinne, S., Kondo, Y., Quinn, P. K.,
737 Sarofim, M. C., Schultz, M. G., Schulz, M., Venkataraman, C., Zhang, H., Zhang, S.,
738 Bellouin, N., Guttikunda, S. K., Hopke, P. K., Jacobson, M. Z., Kaiser, J. W., Klimont,
739 Z., Lohmann, U., Schwarz, J. P., Shindell, D., Storelvmo, T., Warren, S. G. and Zender,
740 C. S.: Bounding the role of black carbon in the climate system: A scientific
741 assessment, J. Geophys. Res. Atmos., 118(11), 5380–5552,
742 doi:10.1002/jgrd.50171, 2013.
743 Cai, H., Burnham, A. and Wang, M.: Updated Emission Factors of Air Pollutants from
744 Vehicle Operations in GREET TM Using MOVES, , (September), 2013.
745 Carslaw, D. C. . and Ropkins, K.: The openair manual open-source tools for analysing
746 air pollution data, King's Coll. London, 27–28(January), 287, 2012.
747 Chung, C. E., Kim, S. W., Lee, M., Yoon, S. C. and Lee, S.: Carbonaceous aerosol AAE
748 inferred from in-situ aerosol measurements at the Gosan ABC super site, and the
749 implications for brown carbon aerosol, Atmos. Chem. Phys., 12(14), 6173–6184,
750 doi:10.5194/acp-12-6173-2012, 2012.
751 Crutzen, P. J. and Andreae, M.: Biomass Burning in the Tropics : Impact on
752 Atmospheric Chemistry and Biogeochemical Cycles Estimates of Worldwide
753 Biomass Burning, Science (80-.)., 250(4988), 1669–1678,
754 doi:10.1126/science.250.4988.1669, 1990.
755 Dickerson, R. R., Andreae, M. O., Campos, T., Mayol-Bracero, O. L., Neususs, C. and
756 Streets, D. G.: Analysis of black carbon and carbon monoxide observed over the
757 Indian Ocean: Implications for emissions and photochemistry, J. Geophys. Res.,
758 107(D19), doi:Artn 8017\rDoi 10.1029/2001jd000501, 2002.
759 Drinovec, L., Močnik, G., Zotter, P., Prévôt, A. S. H., Ruckstuhl, C., Coz, E., Rupakheti, M.,
760 Sciare, J., Müller, T., Wiedensohler, A. and Hansen, A. D. A.: The "dual-spot"
761 Aethalometer: An improved measurement of aerosol black carbon with real-time
762 loading compensation, Atmos. Meas. Tech., 8(5), 1965–1979, doi:10.5194/amt-8-
763 1965-2015, 2015.
764 Dumka, U. C., Manchanda, R. K., Sinha, P. R., Sreenivasan, S., Moorthy, K. K. and Suresh

765 Babu, S.: Temporal variability and radiative impact of black carbon aerosol over
766 tropical urban station Hyderabad, J. Atmos. Solar-Terrestrial Phys., 105–
767 106(April 2016), 81–90, doi:10.1016/j.jastp.2013.08.003, 2013.
768 Field, R. D., van der Werf, G. R., Fanin, T., Fetzer, E. J., Fuller, R., Jethva, H., Levy, R.,
769 Livesey, N. J., Luo, M., Torres, O. and Worden, H. M.: Indonesian fire activity and
770 smoke pollution in 2015 show persistent nonlinear sensitivity to El Niño-induced
771 drought, Proc. Natl. Acad. Sci., 113(33), 9204–9209,
772 doi:10.1073/pnas.1524888113, 2016.
773 Food and Agriculture Organization of the United Nations: What woodfuels can do to
774 mitigate climate change, FAO For. Pap., 98, 2010.
775 Galbraith, K.: Measuring Africa's Air Pollution, New York Times, 16th April [online]
776 Available from: http://www.nytimes.com/2014/04/17/business/energy-
777 environment/measuring-africas-air-pollution.html?_r=0, 2014.
778 Garg, S., Chandra, B. P., Sinha, V., Sarda-Esteve, R., Gros, V. and Sinha, B.: Limitation of
779 the Use of the Absorption Angstrom Exponent for Source Apportionment of
780 Equivalent Black Carbon: a Case Study from the North West Indo-Gangetic Plain,
781 Environ. Sci. Technol., 50(2), 814–824, doi:10.1021/acs.est.5b03868, 2016.
782 Gasore, J.: Quantifying Emissions of Carbon Dioxide and Methane in Central and
783 Eastern Africa Through High Frequency Measurements and Inverse Modeling,
784 Massachusetts Institute of Technology., 2018.
785 Gatari, M. J. and Boman, J.: Black carbon and total carbon measurements at urban and
786 rural sites in Kenya, East Africa, Atmos. Environ., 37(8), 1149–1154,
787 doi:10.1016/S1352-2310(02)01001-4, 2003.
788 Harrison, R. M., Beddows, D. C. S., Hu, L. and Yin, J.: Comparison of methods for
789 evaluation of wood smoke and estimation of UK ambient concentrations, Atmos.
790 Chem. Phys., 12(17), 8271–8283, doi:10.5194/acp-12-8271-2012, 2012.
791 Hersey, S. P., Garland, R. M., Crosbie, E., Shingler, T., Sorooshian, A., Piketh, S. and
792 Burger, R.: An overview of regional and local characteristics of aerosols in South
793 Africa using satellite, ground, and modeling data, Atmos. Chem. Phys., 15(8),
794 4259–4278, doi:10.5194/acp-15-4259-2015, 2015.
795 Hsu, Y. K., Holsen, T. M. and Hopke, P. K.: Comparison of hybrid receptor models to
796 locate PCB sources in Chicago, Atmos. Environ., 37(4), 545–562,
797 doi:10.1016/S1352-2310(02)00886-5, 2003.
798 IHME: GBD Compare Data Visualization, Inst. Heal. Metrics Eval. Seattle, WA IHME,
799 Univ. Washingt., 2016.
800 Kabashnikov, V. P., Chaikovsky, A. P., Kucsera, T. L. and Metelskaya, N. S.: Estimated
801 accuracy of three common trajectory statistical methods, Atmos. Environ., 45(31),
802 5425–5430, doi:10.1016/j.atmosenv.2011.07.006, 2011.
803 Kalnay, E., Kanamitsu, M., Kistler, R., Collins, W., Deaven, D., Gandin, L., Iredell, M.,
804 Saha, S., White, G., Woollen, J., Zhu, Y., Chelliah, M., Ebisuzaki, W., Higgins, W.,
805 Janowiak, J., Mo, K. C., Ropelewski, C., Wang, J., Leetmaa, A., Reynolds, R., Jenne, R.
806 and Joseph, D.: The NCEP/NCAR 40-year reanalysis project, Bull. Am. Meteorol.
807 Soc., 77(3), 437–471, doi:10.1175/1520-0477(1996)077<0437:TNYRP>2.0.CO;2,
808 1996.
809 Kinney, P. L., Gichuru, M. G., Volavka-Close, N., Ngo, N., Ndiba, P. K., Law, A., Gachanja,
810 A., Gaita, S. M., Chillrud, S. N. and Sclar, E.: Traffic impacts on PM2.5 air quality in

Nairobi, Kenya, Environ. Sci. Policy, 14(4), 369–378, doi:10.1016/j.envsci.2011.02.005, 2011.

Kirchstetter, T. W. and Thatcher, T. L.: Contribution of organic carbon to wood smoke particulate matter absorption of solar radiation, Atmos. Chem. Phys., 12(14), 6067–6072, doi:10.5194/acp-12-6067-2012, 2012.

Knippertz, P., Coe, H., Chiu, J. C., Evans, M. J., Fink, A. H., Kalthoff, N., Liousse, C., Mari, C., Allan, R. P., Brooks, B., Danour, S., Flamant, C., Jegede, O. O., Lohou, F. and Marsham, J. H.: The dacciwa project: Dynamics-aerosol-chemistry-cloud interactions in West Africa, Bull. Am. Meteorol. Soc., 96(9), 1451–1460, doi:10.1175/BAMS-D-14-00108.1, 2015.

Koch, D., Schulz, M., Kinne, S., McNaughton, C., Spackman, J. R., Balkanski, Y., Bauer, S., Berntsen, T., Bond, T. C., Boucher, O., Chin, M., Clarke, A., De Luca, N., Dentener, F., Diehl, T., Dubovik, O., Easter, R., Fahey, D. W., Feichter, J., Fillmore, D., Freitag, S., Ghan, S., Ginoux, P., Gong, S., Horowitz, L., Iversen, T., Kirkevåg, A., Klimont, Z., Kondo, Y., Krol, M., Liu, X., Miller, R., Montanaro, V., Moteki, N., Myhre, G., Penner, J. E., Perlwitz, J., Pitari, G., Reddy, S., Sahu, L., Sakamoto, H., Schuster, G., Schwarz, J. P., Seland, Ø., Stier, P., Takegawa, N., Takemura, T., Textor, C., van Aardenne, J. a. and Zhao, Y.: Evaluation of black carbon estimations in global aerosol models, Atmos. Chem. Phys., 9(22), 9001–9026, doi:10.5194/acp-9-9001-2009, 2009.

Kuik, F., Lauer, A., Beukes, J. P., Zyl, P. G. Van, Josipovic, M., Vakkari, V., Laakso, L. and Feig, G. T.: The anthropogenic contribution to atmospheric black carbon concentrations in southern Africa : a WRF-Chem modeling study, , 8809–8830, doi:10.5194/acp-15-8809-2015, 2015.

Lack, D. A. and Langridge, J. M.: On the attribution of black and brown carbon light absorption using the aerosol angstrom exponent, Atmos. Chem. Phys., 13(20), 10535–10543, doi:10.5194/acp-13-10535-2013, 2013.

Liousse, C., Assamoi, E., Criqui, P., Granier, C. and Rosset, R.: Explosive growth in African combustion emissions from 2005 to 2030, Environ. Res. Lett., 9(3), 35003, doi:10.1088/1748-9326/9/3/035003, 2014.

Lupu, A. and Maenhaut, W.: Application and comparison of two statistical trajectory techniques for identification of source regions of atmospheric aerosol species, Atmos. Environ., 36(36–37), 5607–5618, doi:10.1016/S1352-2310(02)00697-0, 2002.

Marais, E. A. and Wiedinmyer, C.: Air Quality Impact of Di ff use and Ine ffi cient Combustion Emissions in Africa (DICE-Africa), , doi:10.1021/acs.est.6b02602, 2016.

Mkoma, S. L., Maenhaut, W., Chi, X., Wang, W. and Raes, N.: Characterisation of PM10 atmospheric aerosols for the wet season 2005 at two sites in East Africa, Atmos. Environ., 43(3), 631–639, doi:10.1016/j.atmosenv.2008.10.008, 2009.

Moosmüller, H. and Chakrabarty, R. K.: Technical Note: Simple analytical relationships between Ångström coefficients of aerosol extinction, scattering, absorption, and single scattering albedo, Atmos. Chem. Phys., 11(20), 10677–10680, doi:10.5194/acp-11-10677-2011, 2011.

Ngo, N. S., Gatari, M., Yan, B., Chillrud, S. N., Bouhamam, K. and Kinney, P. L.: Occupational exposure to roadway emissions and inside informal settlements in

sub-Saharan Africa: A pilot study in Nairobi, Kenya, Atmos. Environ., 111, 179–184, doi:10.1016/j.atmosenv.2015.04.008, 2015.

Niang, I., Ruppel, O. C., Abdrabo, M. A., Essel, A., Lennard, C., Padgham, J. and Urquhart, P.: Africa, Clim. Chang. 2014 Impacts, Adapt. Vulnerability - Contrib. Work. Gr. II to Fifth Assess. Rep. Intergov. Panel Clim. Chang., 1199–1265, doi:10.1017/CBO9781107415386.002, 2014.

Pan, X. L., Kanaya, Y., Wang, Z. F., Liu, Y., Pochanart, P., Akimoto, H., Sun, Y. L., Dong, H. B., Li, J., Irie, H. and Takigawa, M.: Correlation of black carbon aerosol and carbon monoxide in the high-altitude environment of Mt. Huang in Eastern China, Atmos. Chem. Phys., 11(18), 9735–9747, doi:10.5194/acp-11-9735-2011, 2011.

Prinn, R. G., Weiss, R. F., Fraser, P. J., Simmonds, P. G., Cunnold, D. M., Alyea, F. N., O'Doherty, S., Salameh, P., Miller, B. R., Huang, J., Wang, R. H. J., Hartley, D. E., Harth, C., Steele, L. P., Sturrock, G., Midgley, P. M. and McCulloch, A.: A history of chemically and radiatively important gases in air deduced from ALE/GAGE/AGAGE, J. Geophys. Res. Atmos., 105(D14), 17751–17792, doi:10.1029/2000JD900141, 2000.

Ramanathan, V. and Carmichael, G.: Global and regional climate changes due to black carbon, Nat. Geosci., 1, 221–227, doi:10.1038/ngeo156, 2008.

Real, E., Orlandi, E., Law, K. S., Fierli, F., Josset, D., Cairo, F., Schlager, H., Borrmann, S., Kunkel, D., Volk, C. M., McQuaid, J. B., Stewart, D. J., Lee, J., Lewis, A. C., Hopkins, J. R., Ravegnani, F., Ulanovski, A. and Liousse, C.: Cross-hemispheric transport of central African biomass burning pollutants: Implications for downwind ozone production, Atmos. Chem. Phys., 10(6), 3027–3046, doi:10.5194/acpd-9-17385-2009, 2010.

Russell, P. B., Bergstrom, R. W., Shinozuka, Y., Clarke, a. D., DeCarlo, P. F., Jimenez, J. L., Livingston, J. M., Redemann, J., Holben, B., Dubovik, O. and Strawa, A.: Absorption Angstrom Exponent in AERONET and related data as an indicator of aerosol composition, Atmos. Chem. Phys., 10, 1156–1169, doi:10.5194/acpd-9-21785-2009, 2010.

Rwanda, R. of: Energy Sector Strategic Plan: Republic of Rwanda Ministry of Infrastructure, Kigali, Rwanda., 2015.

Saarikoski, S., Carbone, S., Decesari, S., Giulianelli, L., Angelini, F., Canagaratna, M., Ng, N. L., Trimborn, a., Facchini, M. C., Fuzzi, S., Hillamo, R. and Worsnop, D.: Chemical characterization of springtime submicrometer aerosol in Po Valley, Italy, Atmos. Chem. Phys., 12(18), 8401–8421, doi:10.5194/acp-12-8401-2012, 2012.

Sahu, L. K., Kondo, Y., Moteki, N., Takegawa, N., Zhao, Y., Cubison, M. J., Jimenez, J. L., Vay, S., Diskin, G. S., Wisthaler, A., Mikoviny, T., Huey, L. G., Weinheimer, A. J. and Knapp, D. J.: Emission characteristics of black carbon in anthropogenic and biomass burning plumes over California during ARCTAS-CARB 2008, J. Geophys. Res. Atmos., 117(16), 1–20, doi:10.1029/2011JD017401, 2012.

Saleh, R., Hennigan, C. J., McMeeking, G. R., Chuang, W. K., Robinson, E. S., Coe, H., Donahue, N. M. and Robinson, A. L.: Absorptivity of brown carbon in fresh and photo-chemically aged biomass-burning emissions, Atmos. Chem. Phys., 13(15), 7683–7693, doi:10.5194/acp-13-7683-2013, 2013.

Saleh, R., Robinson, E. S., Tkacik, D. S., Ahern, A. T., Liu, S., Aiken, A. C., Sullivan, R. C., Presto, A. a., Dubey, M. K., Yokelson, R. J., Donahue, N. M. and Robinson, A. L.:

Brownness of organics in aerosols from biomass burning linked to their black carbon content, Nat. Geosci., 7(September), 1–4, doi:10.1038/ngeo2220, 2014.

Sandradewi, J., Prévôt, A. S. H., Szidat, S., Perron, N., Alfarra, M. R., Lanz, V. A., Weingartner, E. and Baltensperger, U.: Using Aerosol Light Absorption Measurements for the Quantitative Determination of Wood Burning and Traffic Emission Contributions to Particulate Matter, Environ. Sci. Technol., 42(9), 3316–3323, doi:10.1021/es702253m, 2008.

Sauvage, B., Thouret, V., Cammas, J. P., Gheusi, F., Athier, G. and Nédélec, P.: Tropospheric ozone over Equatorial Africa: regional aspects from the MOZAIC data, Atmos. Chem. Phys., 5, 311–335, doi:10.5194/acpd-4-3285-2004, 2005.

Seibert, P., Kromp-Kolb, H., Baltensperger, U., Jost, D. T. and Schwikowski, M.: Trajectory Analysis of High-Alpine Air Pollution Data, in Air Pollution Modeling and Its Application: NATO: Challenges of Modern Society, edited by S.-E. (Riso N. L. Gryning and M. M. (Centre for E. S. of the M. Millan, pp. 595–596, Springer USA., 1994.

Thompson, A. M., Diab, R. D., Bodeker, G. E., Zunckel, M., Coetzee, G. J. R., Archer, C. B., Mcnamara, D. P., Pickering, K. E., Combrink, J., Fishman, J. and Nganga, D.: Ozone over southern Africa during SAFARI-92 / TRACE A, , 101(95), 1996.

Tiitta, P., Vakkari, V., Croteau, P., Beukes, J. P., Van Zyl, P. G., Josipovic, M., Venter, A. D., Jaars, K., Pienaar, J. J., Ng, N. L., Canagaratna, M. R., Jayne, J. T., Kermi, V. M., Kokkola, H., Kulmala, M., Laaksonen, A., Worsnop, D. R. and Laakso, L.: Chemical composition, main sources and temporal variability of PM1 aerosols in southern African grassland, Atmos. Chem. Phys., 14(4), 1909–1927, doi:10.5194/acp-14-1909-2014, 2014.

van Vliet, E. D. S. and Kinney, P. L.: Impacts of roadway emissions on urban particulate matter concentrations in sub-Saharan Africa: new evidence from Nairobi, Kenya, Environ. Res. Lett., 2(4), 45028, doi:10.1088/1748-9326/2/4/045028, 2007.

Welp, L. R., Keeling, R. F., Weiss, R. F., Paplawsky, W. and Heckman, S.: Design and performance of a Nafion dryer for continuous operation at CO2and CH4 air monitoring sites, Atmos. Meas. Tech., 6(5), 1217–1226, doi:10.5194/amt-6-1217-2013, 2013.

WHO: Health Effects of Particulate Matter: Policy imlications for countries in eastern Europe, Caucasus and central Asia, World Heal. Organ., 15 [online] Available from: www.euro.who.int, 2013.

World Bank: World Development Report 2011: World Development Indicators, Fossil Fuel Energy Consumption., 2011.

Yuan, J. F., Huang, X. F., Cao, L. M., Cui, J., Zhu, Q., Huang, C. N., Lan, Z. J. and He, L. Y.: Light absorption of brown carbon aerosol in the PRD region of China, Atmos. Chem. Phys., 16(3), 1433–1443, doi:10.5194/acp-16-1433-2016, 2016.

Zhang, L., Jin, L., Zhao, T., Yin, Y., Zhu, B., Shan, Y., Guo, X., Tan, C., Gao, J. and Wang, H.: Diurnal variation of surface ozone in mountainous areas: Case study of Mt. Huang, East China, Sci. Total Environ., 538, 583–590, doi:10.1016/j.scitotenv.2015.08.096, 2015.

Zhang, Y., Cooper, O. R., Gaudel, A., Thompson, A. M., Nédélec, P., Ogino, S. and West, J. J.: Tropospheric ozone change from 1980 to 2010 dominated by equatorward redistribution of emissions, Nat. Geosci., 9(December), 875–881,

949 doi:10.1038/NGEO2827, 2016.
950
951

Atmos. Chem. Phys. Discuss., https://doi.org/10.5194/acp-2018-100
Manuscript under review for journal Atmos. Chem. Phys.
Discussion started: 2 February 2018

952 **Figure 1**. From top left moving counter-clockwise: an aerial view of RCO at Mt.

953 Mugogo Main Peak, the station with towers in the background, and the location of Mt.

954 Mugogo in Rwanda (blue pin) in relation to Kigali (yellow pin).

955

Atmos. Chem. Phys. Discuss., https://doi.org/10.5194/acp-2018-100
Manuscript under review for journal Atmos. Chem. Phys.
Discussion started: 2 February 2018

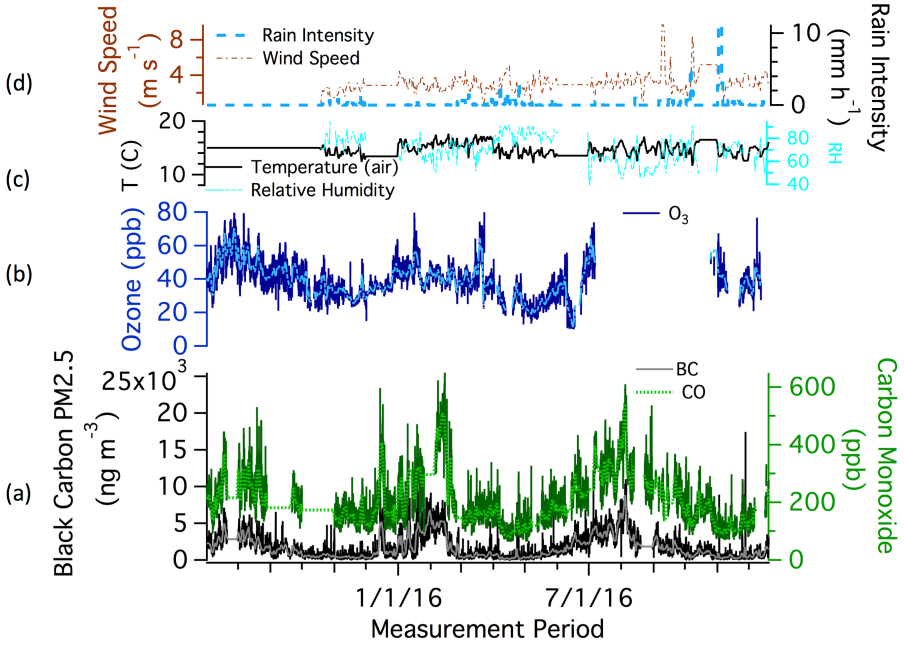

Figure 2. From the bottom up: (a) black carbon (black, grey) and carbon monoxide (dark green, light green) (15 minute, daily) average concentrations; (b) ozone (dark blue, light blue) (15 minute, daily), (c) temperature (black) and relative humidity (light blue) values; (d) wind speed (red dotted) and rain intensity (blue dash) daily average values.

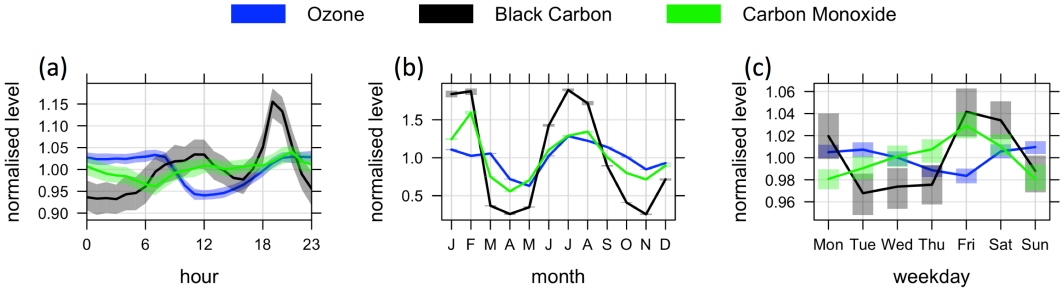

Figure 3. Normalized temporal variations of O_3 mixing ratios, CO mixing ratios, and BC concentrations: (a) diurnal (b) monthly concentrations, and (c) differences by day of the week. Shaded areas are 95% confidence intervals.

Atmos. Chem. Phys. Discuss., https://doi.org/10.5194/acp-2018-100
Manuscript under review for journal Atmos. Chem. Phys.
Discussion started: 2 February 2018

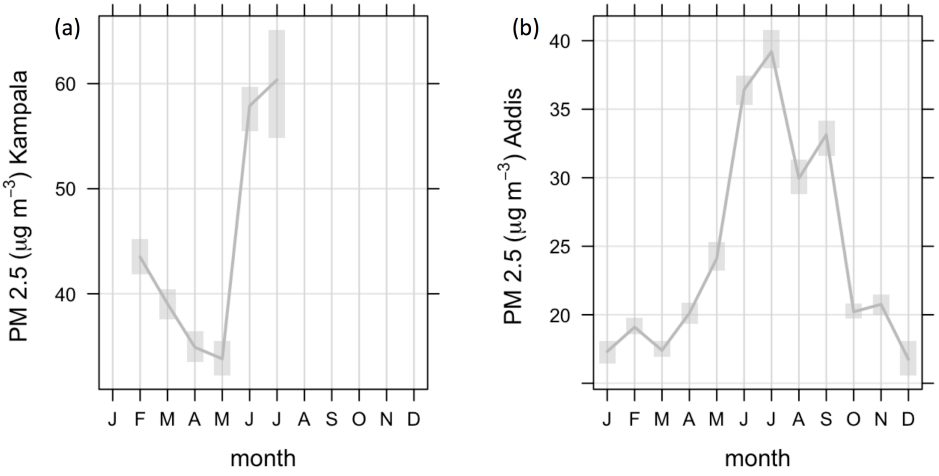

Figure 4: Monthly means of PM2.5 concentrations measured at the US Embassies in (**a**) Kampala, Uganda and (**b**) Addis Ababa, Ethiopia (right) from January-December 2016/2017 (as available). Shaded areas are 95% confidence intervals.

Atmos. Chem. Phys. Discuss., https://doi.org/10.5194/acp-2018-100
Manuscript under review for journal Atmos. Chem. Phys.
Discussion started: 2 February 2018

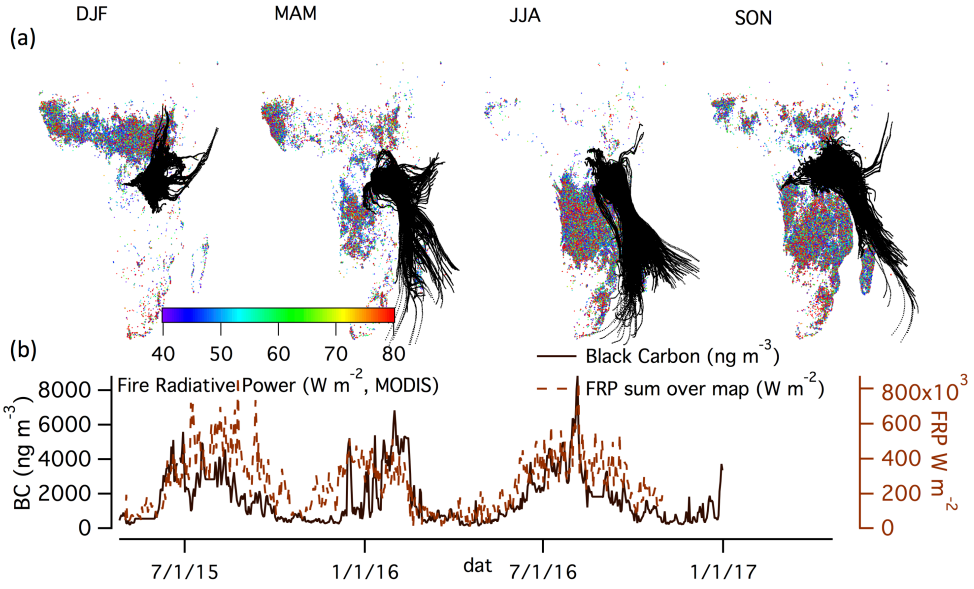

Figure 5. (a) Seasonal fire radiative power data acquired with the MODIS instrument and back trajectories of air masses (generated with the HYSPLIT model) reaching the Rwanda Climate Observatory for the period May 2015 to January 2017. Seasons in Rwanda are split into: short dry season, December-January-February (DJF), long rainy season, March-April-May (MAM), long dry season, June-July-August (JJA,) and short rainy season, September-October-November (SON). (b) The time series of daily average BC concentration and the daily sum of Fire Radiative Power (W m^{-2}) from the pictured data bound by the furthest HYSPLIT backtrajectory reaches each season (box defined by the most north, south, east, and west point the HYSPLIT backtrajectories reach).

Atmos. Chem. Phys. Discuss., https://doi.org/10.5194/acp-2018-100
Manuscript under review for journal Atmos. Chem. Phys.
Discussion started: 2 February 2018

Atmospheric Chemistry and Physics Discussions

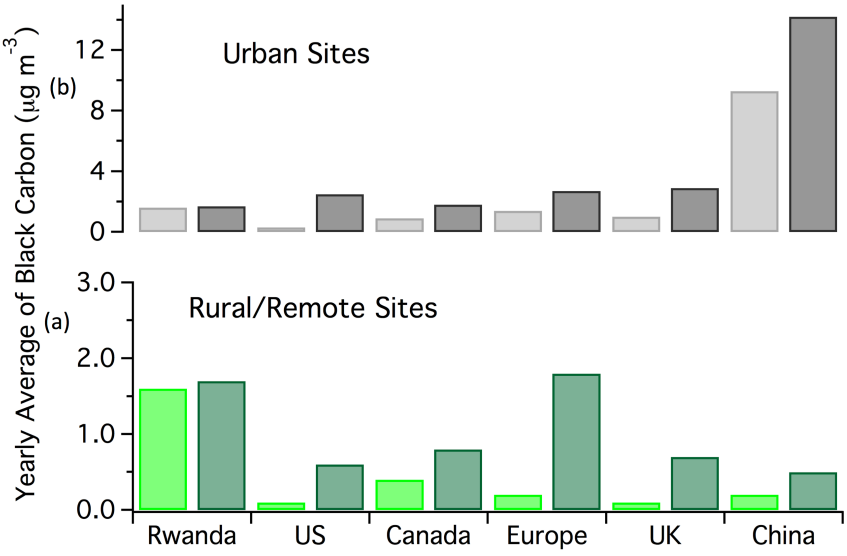

Figure 6. (a) Urban and (b) rural maximum (dark grey/green) of annual averages (dark grey/green) and minimum (light grey/green) of annual averages (light grey/green) BC concentrations at various sites globally. The BC data for Rwanda is from one location (Mt. Mugogo, rural), while the data for other locations were from multiple locations, averaged over one year. The annual average BC concentrations for Rwanda were calculated for the data from April 1st to April 1st of the next year. There was BC data for two years measured at RCO. BC data source for other sites: https://www3.epa.gov/blackcarbon/2012report/Chapter5.pdf, compiled from multiple sources.

Atmos. Chem. Phys. Discuss., https://doi.org/10.5194/acp-2018-100
Manuscript under review for journal Atmos. Chem. Phys.
Discussion started: 2 February 2018

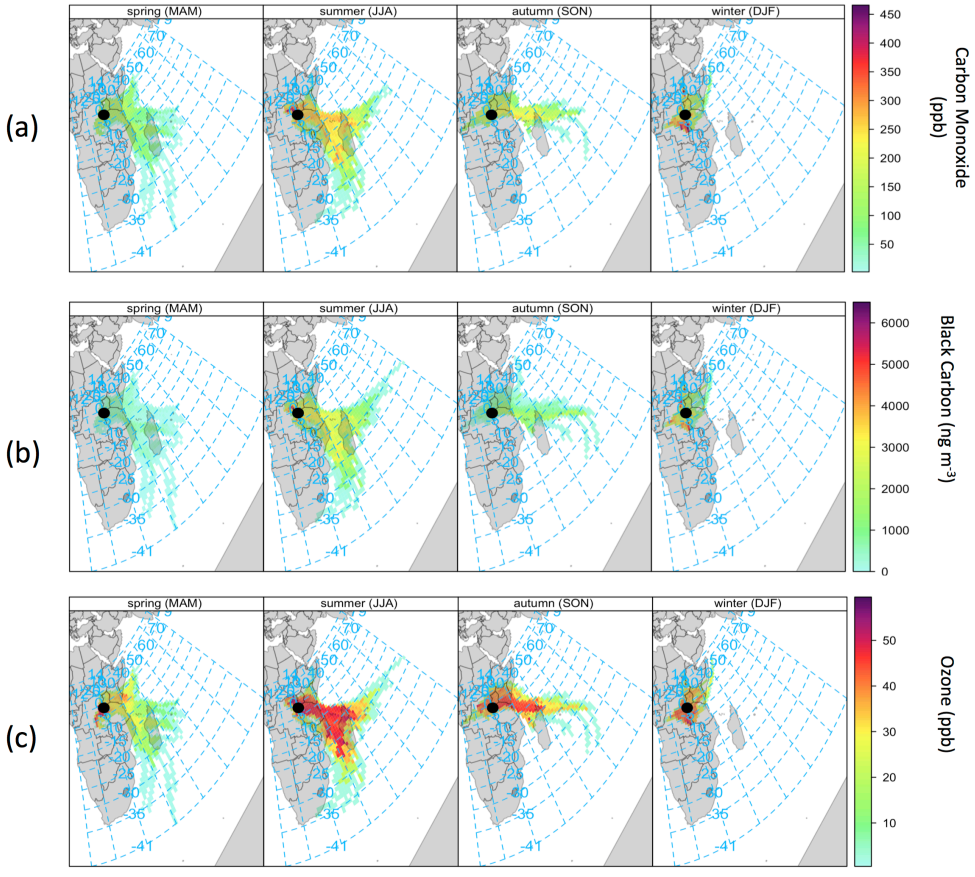

Figure 7. From top to bottom, concentration-weighted back trajectories of (a) CO, (b) BC, and (c) O_3, separated by season, for measurements at the Rwanda Climate Observatory (black dot) for the period of July 2015-January 2017.

Atmos. Chem. Phys. Discuss., https://doi.org/10.5194/acp-2018-100
Manuscript under review for journal Atmos. Chem. Phys.
Discussion started: 2 February 2018

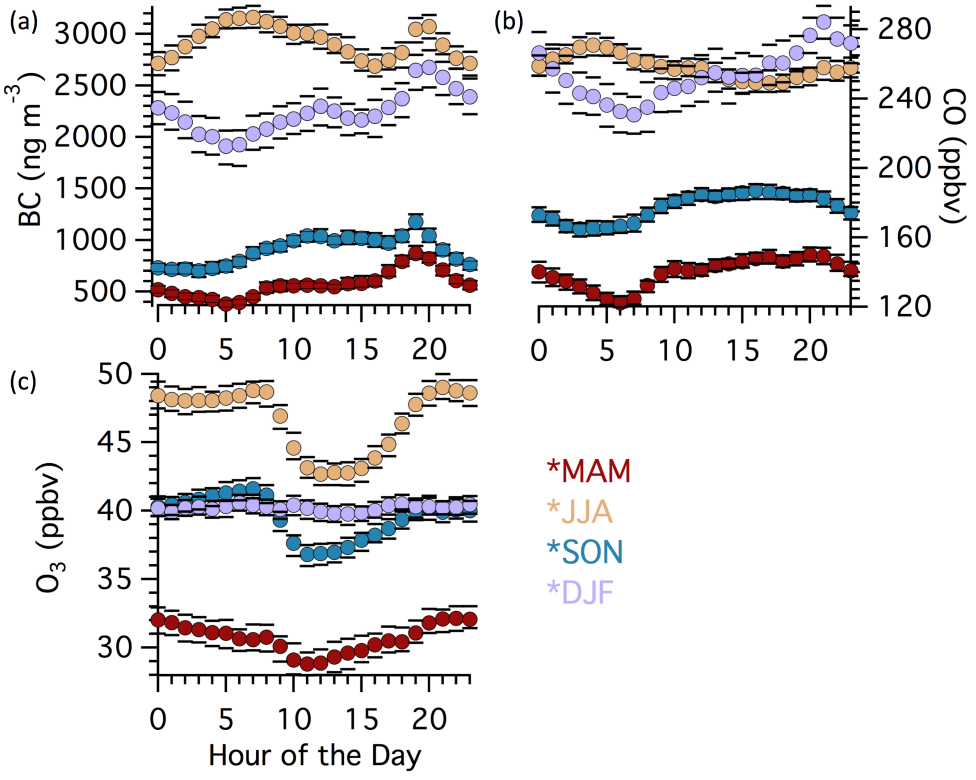

Figure 8. Seasonally separated diurnal profiles of (a) BC concentrations, (b) CO mixing ratios, and (c) O_3 mixing ratios, colored for each season. The circles represent mean concentrations and the lines represent 95% confidence intervals.

Atmos. Chem. Phys. Discuss., https://doi.org/10.5194/acp-2018-100
Manuscript under review for journal Atmos. Chem. Phys.
Discussion started: 2 February 2018

Atmospheric Chemistry and Physics Discussions

1048

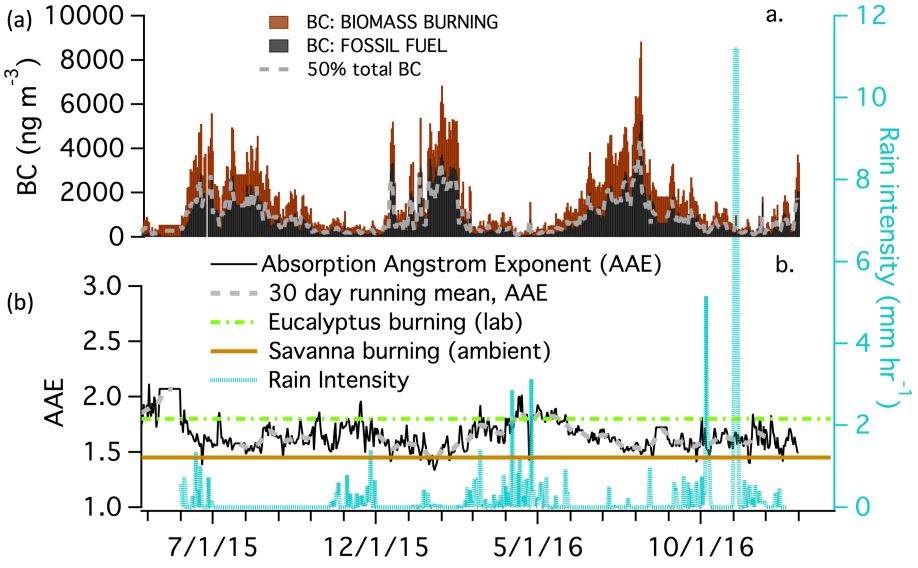

1049 **Figure 9**. (a) Time series of contributions of fossil fuel combustion and biomass
1050 burning to BC concentrations observed at RCO. (b) Daily average absorption
1051 Angstrom exponent (AAE) measured at RCO (black line), rain intensity, and published
1052 AAE for Eucalyptus burning ((Yuan et al., 2016), laboratory studies, green line) and
1053 savanna burning ((Russell et al., 2010), ambient, brown line) also shown as reference.

1054